A continuous modeling approach for describing the atomization process from inside the injector to the final spray

G. Blokkeel[1], A. Mura[2], F-x. Demoulin[3] and R. Borghi[4]

1. PSA Peugeot Citroën. Route de Gisy, 78943 Vélizy-Villacoublay Cedex, France
2. CORIA-CNRS , Saint Etienne du Rouvray cedex 76801, FRANCE
3. CORIA-University of Rouen, Saint Etienne du Rouvray cedex 76801, France
4. LMA-ESM2, Marseille, France

There is a great necessity to reach higher efficiency in many industrial devices like rocket engine or automotive engine; solutions essentially go through a better control of the atomization process. To avoid numerous expensive experiments, numerical simulation is called to play an important role. However despite the important effort spend to understand and model the atomization process, the models used in CFD code are not accurate enough to be predictive in the domain of spray formation. This is mainly due to the weaknesses that suffer the description of the primary breakup zone that is generally not integrated and computed in CFD simulations. Following the pioneering work of Vallet et al [1-2], we present here a model for the primary breakup that permits to describe continuously the liquid behavior from inside the injector to the end of the spray formation. The model relies on the hypothesis of high Reynolds and Weber number. Under these assumptions, the behavior of the liquid jet at large scale is driven by turbulent characteristic: the dispersion of the liquid is due to mean liquid turbulent mass flux. Both viscosity and surface tension act only on small scales and are responsible for the formation of final droplets. This effect is taken into account by using an equation for the mean liquid-gas surface density. Due to the strong interaction between the liquid and gas, during the primary breakup, there are difficulties to consider separately each phase or to describe the evolution of Lagrangian fluid particles. Hence, an Eulerian description of a unique phase containing both liquid and gas is used. Finally, at every points where the liquid volume fraction is small enough a Lagrangian stochastic description of the spray is initialized in order to benefit from the important background accumulated using this method on diluted spray. The necessary adaptation of the turbulent modeling for such flow composed by liquid and gas, together with the improvements obtained by a continuous description of the atomization are the main points described in this paper.

1. Introduction

In many industrial devices, it is necessary to mix a liquid fluid together with a gas. This is usually achieved by atomizing the liquid in order to form droplets small enough to be vaporized quickly. The atomizer system must be able to form spray with prescribed characteristics like mean droplet diameters, penetration length, size distribution and so on. Even when an atomizer is calibrated accurately for a certain set of conditions, it is used in an unknown environment in the final process, for example the turbulent flow within the combustion chamber of Diesel engine. Since these external conditions can affect the spray characteristics it is necessary to develop predictive atomization models to prevent numerous experiments: one for each possible external condition.

Because the external environment plays a role during the atomization process a necessary characteristic of the model must be its ability to describe the whole process continuously to permit that outside medium can affect the atomization. The difficulty of this task concerns the primary breakup that takes place just at the exit of the injector which corresponds generally to a mixture of gas and liquid where both liquid and gas are present in similar proportion. Due to a high quantity of liquid-gas interface, this dense part of the spray is difficult to attain both numerically (necessity to represent the interfacial characteristics) and experimentally (laser diagnostics are usually handicapped by multi diffusion and reflection effects that take place at the interface).
Usually the modeling of the primary and the secondary break-up are considered separately. The primary break-up consists in the atomization process that takes place inside the injector to the dense part of the spray. The secondary break-up describes how the parcels of liquid initially formed are transformed to a dilute spray, composed by small spherical droplets. The primary break-up is usually not computed, thus the initial blobs of liquid are injected with a priori characteristics, for example in many model the initial size of the blobs are supposed to be related to the injector diameter [3]. The positions where these big blobs are injected in the gas flow can be at the injector tip or if a liquid core is expected along a cone based on the injector tip, but the place of injection must be determined previously by empirical means.
With such representation of the atomization most of the works were focused on the secondary break-up. Since the liquid is considered as a set of dispersed droplets a Lagrangian stochastic particle description of the liquid phase is generally used. The advantage of this method is that most of the phenomena linked to each droplet (drag, vaporization, heating, …) can be depicted by considering the case of a unique droplet in an infinite gas phase.
Here, the description of the dense part of the spray is addressed by using a model initially proposed by Vallet et *al.* [2]. This model is designed to describe the atomization for flows at high Reynolds and Weber number, such flows are of interest for many practical devices where it is needed to obtain quickly very small droplets as it is the case for Diesel fuel injection and for rocket fuel injection. The dense part of the spray is a turbulent mixture of liquid and gas where the interactions between both phases are too strong to consider each phase independently. Since these interactions are strong and complex it is advantageous to consider the whole mixture as a unique turbulent flow containing two species the gas and the liquid. Therefore a one flow Eulerian representation is used, remark that representation does not imply that the mean liquid velocity and gas velocity are identical [2]. Initially just at the exit of the injector the inertial forces are so important that both surface tension and viscous forces do not play a role on the initial dispersion of the liquid that is mainly due to a turbulent mass flux. Such turbulence in a flow with very high-density fluctuations (from the gas density to the liquid density) can have particular behavior and must be studied particularly. But to know the size of the droplets, which are the smallest scales of the liquid parcels, an equation for the liquid-gas surface density is used and this allows to represent the effect of the surface tension.
A general overview of the approach will be described in the first part. In the second part we will show the need for a particular modeling of the turbulence in such flow. Finally the potential of the whole model will be demonstrated by recent results on coupling inside injector calculations to the computation of the atomization process.

2. General presentation of the model

The classical single-phase $k-\varepsilon$ turbulence model or the Reynolds stress model adapted for such a flow will be used. Here the definition of k or ε does not distinguish the liquid from

the gas phase. Despite the single-phase approach the mean velocity or the turbulence of the liquid can still be derived from the model [4].
As we study the mixture of liquid and gas, the transport equation for the mean velocity does not contain any momentum exchange terms between the two phases, and can therefore be derived as usual:

$$\frac{\partial \overline{\rho u_i}}{\partial t} + \frac{\partial \overline{\rho u_j u_i}}{\partial x_j} = -\frac{\partial \overline{p}}{\partial x_i} + \frac{\partial - \overline{\rho u''_j u''_i}}{\partial x_j} \tag{1}$$

The evolution of the liquid concentration is described by a classical transport equation for the liquid mass fraction:

$$\frac{\partial \overline{\rho Y_l}}{\partial t} + \frac{\partial \overline{\rho u_j Y_l}}{\partial x_j} = \frac{\partial - \overline{\rho u''_j Y''_l}}{\partial x_j} \tag{2}$$

The Reynolds stress tensor model and the turbulent liquid mass flux will be discussed further (see section 3). The following statement will allow us to link together the mean density and the mean liquid mass fraction. The liquid density is always assumed to be constant, if the gas density can be considered as constant too, it is found that:

$$\frac{1}{\overline{\rho}} = \frac{\widetilde{Y}_l}{\rho_l} + \frac{1-\widetilde{Y}_l}{\rho_g}, \tag{3}$$

for gas with variable density, the gas density is linked to the mean pressure by:

$$\overline{p} = \frac{\overline{\rho}\left(1-\widetilde{Y}_l\right)R_g T_g}{1-\overline{\rho}\,\widetilde{Y}_l/\rho_l}, \text{ where } T_g \text{ stays for the mean gas temperature.} \tag{4}$$

The volume fraction of liquid is given by: $\overline{\phi_l} = \dfrac{\overline{\rho Y_l}}{\rho_l}$. (5)

A critical Weber number can be considered to determine the size of the droplets by assuming equilibrium between the surface tension forces and the inertial forces caused by turbulent motion. To avoid this assumption, a transport equation for the mean liquid-gas surface density $\overline{\Sigma}$ is considered [2]. The Sauter mean diameter is proportional to the ratio $\widetilde{Y}_l/\overline{\Sigma}$. As for the transport equation for the flame surface density [5], an equation for $\overline{\Sigma}$ is postulated. The equation can be derived as follows:

$$\frac{\partial \overline{\Sigma}}{\partial t} + \frac{\partial \widetilde{u}_j \overline{\Sigma}}{\partial x_j} = \frac{\partial}{\partial x_j}\left(D_t \frac{\partial \overline{\Sigma}}{\partial x_j}\right) + \left(|A| + a_{coll}\right).\overline{\Sigma} - V_s.\overline{\Sigma}^2 \tag{6}$$

$$A = \alpha_0 \frac{\overline{\rho u''_i u''_j}}{\overline{\rho} k} \frac{\partial \widetilde{u}_i}{\partial x_j}, \text{ a production term due to the mean flow stretching} \tag{7}$$

$$a_{coll} = \frac{\alpha_1}{(36\pi)^{2/9}} \left(l_t \overline{\Sigma}\right)^{2/3} \left(\frac{\rho_l}{\overline{\rho}\widetilde{Y}_l}\right)^{4/9} \frac{\varepsilon}{k}, \text{ a small scale production term due to collision effects} \tag{8}$$

$$V_s = \frac{a_{coll}\rho_l r_{eq}}{3\overline{\rho}\widetilde{Y}_l}, \text{ destruction term due to coalescence, } r_{eq} = C\frac{\sigma^{3/5} l_t^{2/5}}{k} \frac{\left(\overline{\rho}\widetilde{Y}_l\right)^{2/15}}{\rho_l^{11/15}}. \tag{9}$$

The last term, r_{eq}, is the mean equivalent radius of the droplets at the equilibrium.The destruction term is obtained by assuming there is a balance between the collision and coalescence effects. The set of modeling constants used here are: $\alpha_0 = 1.0$, $\alpha_1 = 0.3$, $C = 1.0$, some work is still needed to improve this equation and the validity of the constants.

The whole set of liquid parcels is equivalent to a set of spherical droplets with an equivalent radius: $\overline{r_{32}} = \dfrac{3\overline{\rho Y_l}}{\rho_l \overline{\Sigma}}$ (10)

and an equivalent number of droplets: $n = \dfrac{\rho^2{}_l \overline{\Sigma}^3}{36\pi\left(\overline{\rho Y_l}\right)^2}$. (11)

In this study, the laminar stress tensor is neglected due to the high Reynolds number, and all previous equations are presented without vaporization or combustion terms. The extensions for this case to full reactive flow are discussed in [6].

3. Turbulent dispersion of the liquid

The study of the turbulence model for two-phase flows was conducted in the framework of air-assisted injector. The schematic of such injectors is presented on figure 1 with the main characteristics of the cases studied here:

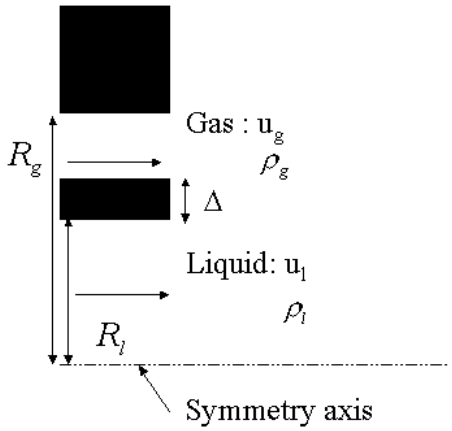

	$\overline{\phi_l}$	LPP(Liquid Presence Probability)		
case	A	B	C	D
u_g	115	175	175	42
ρ_g	1.2	1.2	1.2	10.8
u_l	1.3	2.5	5	2.5
J=$\dfrac{\rho_g u_g^2}{\rho_l u_l^2}$	9.39	5.88	1.47	3.04

Fig 1. Schematic of the air assisted injector

In such injectors the gas velocity is very greater than the liquid velocity. The Reynolds and Weber number based on this velocity difference are high enough to be consistent with the hypothesis of the model. The flow is mainly parabolic except just behind the wall that separates the gas and the liquid flows, where a recirculation zone can be expected. In such flows one of the main characteristic of liquid dispersion is the length of the liquid core that is known to depend mainly on the J number ($J = \rho_g u_g^2 / \rho_l u_l^2$). The experimental result used here are provided by Stepowski et *al* [7] for case A and by Carreau et *al* [8-10] for case B, C and D.

Under these considerations, the turbulence model for flows composed by liquid and gas was studied using a parabolic code [11] assuming that the reciculation zone can be neglected: the dimension Δ of the separating wall is usually very small in comparison to the other dimensions like the initial liquid jet diameter D_l. The first case studied is the case A because the experimental measurement gives us directly the volume liquid fraction $\overline{\phi_l}$.

A second order closure approach using equations for the Reynolds stress tensor and for the liquid turbulent flux $\overline{\rho u''_i Y''_l}$ was initially chosen. The exact equations derived for these quantities contain terms related to the density variations. These terms are usually neglected for gas-gas flow with low-density variation (density ratio lower than ten). For separated flow

(the liquid does not diffuse into the gas) these terms seem to be proportional to $\overline{\rho}\left(1/\rho_l - 1/\rho_g\right)$. Therefore for high-density ratio, as those encounters in a liquid–gas mixture, these terms are expected to be important [2]. A detailed analysis of the different terms have shown [12] that:

- Using the standard $k-\varepsilon$ leads to a big over prediction of the liquid length core (1st order closure).
- The implementation of RSM model with those terms proportional to $\overline{\rho}\left(1/\rho_l - 1/\rho_g\right)$ does not permit to obtain a realistic length for the liquid core (2nd order closure).
- The Prandt number, P_t, used in a $k-\varepsilon$ to model the turbulent liquid mass flux: $\overline{\rho u''_i Y''_l} = -\overline{\rho}\frac{\nu_t}{P_t}\frac{\partial \widetilde{Y}_l}{\partial x_i}$, if it is modified from its usual value 0.9 to 15, that permits to recover a good length of the liquid core but not a profile of the liquid volume fraction comparable to the experimental data (increased 1/Prandt Nb).
- Finally a new formulation of the model for the turbulent liquid mass flux was proposed [13]: $\overline{\rho u''_i Y''_l} = -\overline{\rho}\left(\frac{\nu_t}{P_t} + C_\rho \frac{k^2}{\varepsilon}\overline{\rho}\left(1/\rho_g - 1/\rho_l\right)\right)\frac{\partial \widetilde{Y}_l}{\partial x_i}$, where $C_\rho = 1.8$ (New modeling).

The experimental result is the volume fraction of liquid along the symmetry axis. The measurement in the dense region of the spray is obtained by the fluorescence by a laser sheet of an added substance incorporated in the water [7]. The case A is also characterized by R_g=1.7mm, R_l= 0.9mm, Δ=0.25mm and ρ_l=1000kg/m3. The different models used in the parabolic code are compared to the experimental results on figure 2:

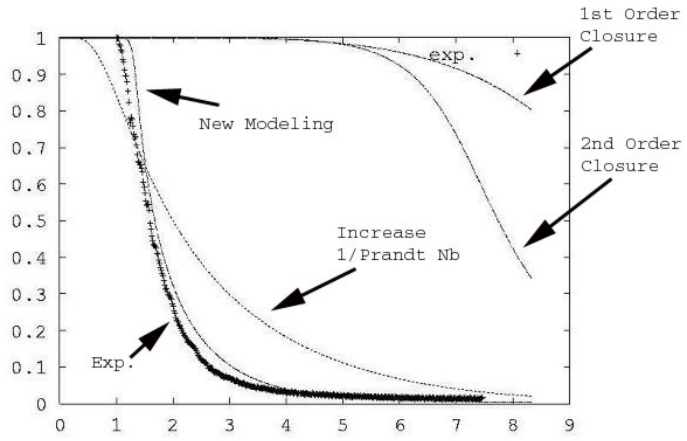

Figure 2. Liquid volume fraction on the injection axis. Experimental results vs. different modeling approaches

Concerning case B, C and D Liquid Presence Probability (LPP) along the axis of the injector is measured using an optic fiber as phase sensor for the liquid phase, see [8-10]. Although it is not clear that the measured LPP is really the volume fraction of the liquid, both are certainly very close when LPP>50%. The characteristics of the experiment are R_g=1.8mm, R_l= 1.05mm, Δ=0.20mm, and ρ_l=1000kg/m3 .

Presented on figure 3 are the results obtained with the original k-ε model and the modified model. The comparison shows that the modification discussed above improves the model prediction, similar trend is found for case D.

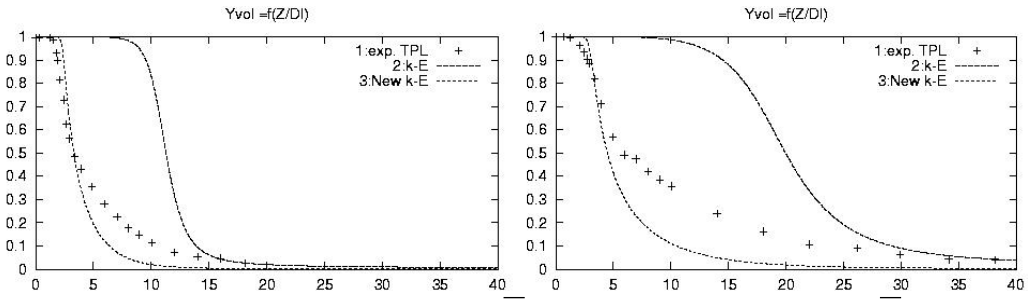

Figure 3. Symbols (1): LPP measurements; $\overline{\phi_l}$ (2) : classical k-ε model, $\overline{\phi_l}$ (3): modified k-ε model. Case B (left) and Case C (right).

The last drawback of the previous modeling concerns the utilization of a parabolic code that is not able to take into account the recirculation zone. To clarify this point the model is implemented in 3D CFD code Fluent [13]. Within this code, the wall between liquid and gas jet is explicitly taken into account in the geometry. The results are presented for the case D on figure 4:

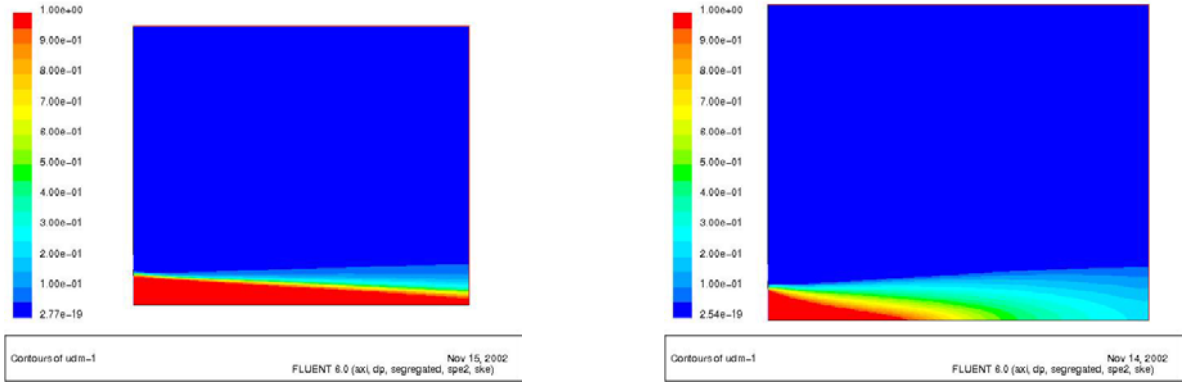

Fig 4: Mean liquid volume fraction field; right: standard k-ε model and left: modified k-ε model.

As with the parabolic code an important difference is found by the utilization of the modified formulation for the turbulent liquid mass flux. The corresponding profiles along the main axis are represented on figure 5:

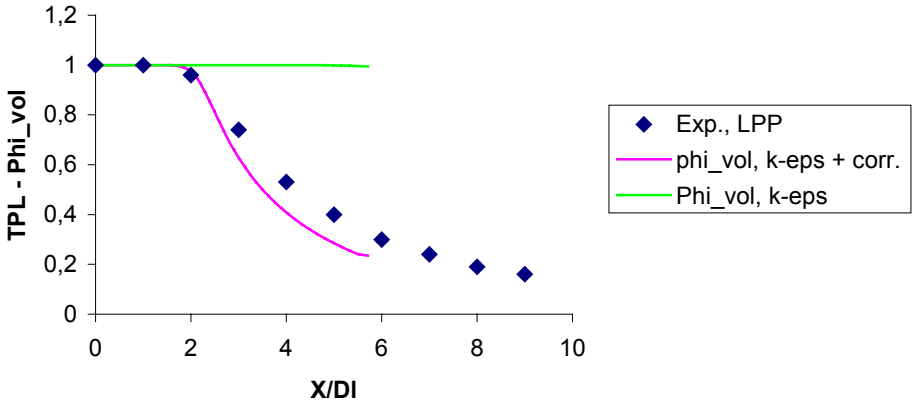

Fig 5: Profiles of LPP measurement and liquid volume fraction numerical results

These profiles seem to confirm the necessity to change the classical modeling for turbulent flows with very high-density fluctuations.

3. Up to the generation of Lagrangian particles representative of the spray

Within this section two applications of the model are shown to demonstrate the improvement obtained by integrating the primary breakup modeling in the CFD computation. The equation for the density of liquid-gas surface per unit of volume is used to permit with the help of the liquid mass fraction to evaluate a mean Sauter radius along the dispersion of the liquid, see equation (10). Dynamically and everywhere in the computational field a criterion is evaluated that compare the mean Sauter diameter to the mean distance between the droplet, $n^{-1/3}$, see equation (11). Wherever this criterion meets a critical value (equal to 2) the model switch from the initial Eulerian single flow formulation to the classical Lagrangian stochastic representation of the spray [4]. Finally for the dense part of the spray the Eulerian formulation is used and for the dilute part the Lagrangian formulation is used, this allows to use the classical models devoted to this part for coalescence, dispersion, vaporization, combustion …

3.1. Influence of the Injector Internal Flow on the Spray for Diesel engine

As shown by several authors [14], for Diesel injection, cavitation or velocity fluctuations inside the injector can significantly modify the spray development inside the combustion chamber. In order to evaluate the influence of these liquid velocity fluctuations, computations done inside the injector [15] are used to provide input conditions. The injection pressure is set at 950 bars and the chamber pressure is equal to 17,5 bars. The injector diameter is 148 μm with a length of 1 mm. The simulation inside the injector is realized with a volume of fluid method. Several points were selected at the exit of the injector to provide us with the different velocity profiles. Because the model is able to take into account the primary breakup zone it is possible to connect continuously the computation inside the injector to the atomization process that takes place outside. The direct effects of the incoming flow fluctuations are shown in comparison with a calculation where the incoming flow is supposed to be perfectly uniform on the figure 6:

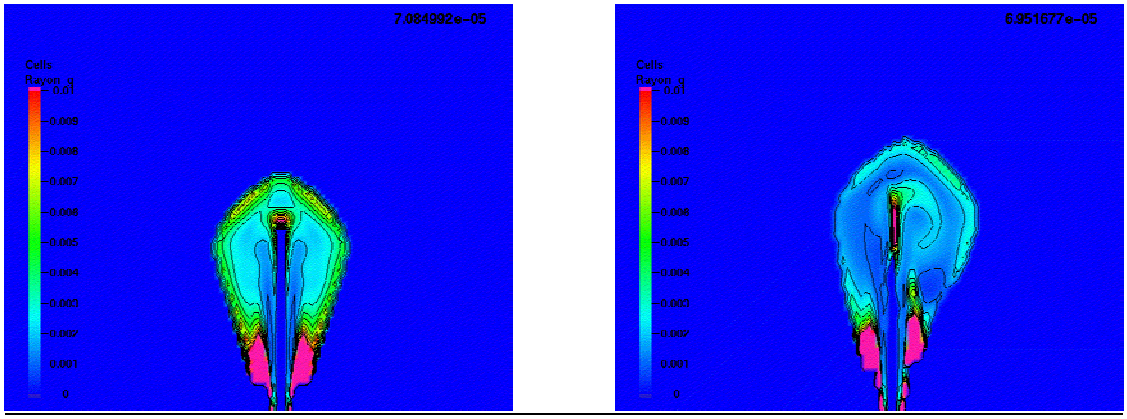

Fig 6. Mean equivalent droplet radii without the injector internal flow coupling (left) and with the injector internal flow coupling (right)

The plots are made during the lift phase of the needle inside the injector. The more obvious results can be seen in the differences in the liquid dispersion. Due to the velocity fluctuations, the spray is no longer symmetric. The sizes of the droplets are also smaller when these fluctuations are taken into account. These results sound physical: by taking into account the

liquid velocity fluctuations, we somewhat perturb the liquid core and this tends to increase the instability of the liquid jet.

3.2 Influence of the Gas Pressure on the Spray Angle

It is well known that the spray angle changes when the gas chamber density changes. The evolution of this angle can be approached by [16]: $\tan(\frac{\Theta}{2}) = 0.7\sqrt{\frac{\rho_g}{\rho_l}}$ (11)

The influence of an elevation of gas density obtained by increasing the pressure is demonstrated on figure 7:

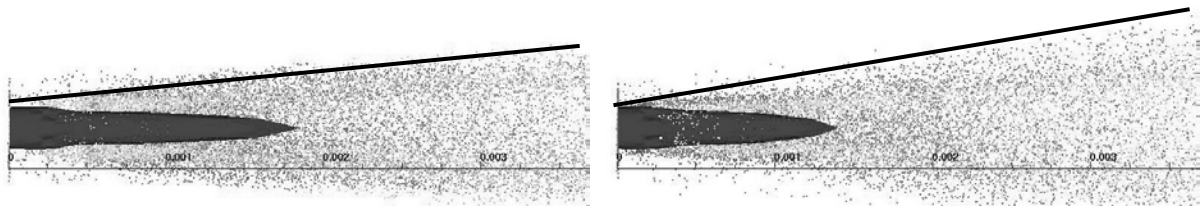

Fig 7: Pressure chamber equal to 10 bars (right), pressure chamber equal to 50 bars (left)

The "reference" half-angles defined by (11) are 4.6 degrees for the 10 bars test-case and around 10 degrees for the 50 bars test-case. For the 10 bar test-case the computation gives about 5 degrees, whereas it gives 9 degrees in the 50 bars test-case.

4. Acknowledgements

The authors acknowledge financial support from CNES, "SNECMA MOTEURS" rocket engine division and PSA Peugeot-Citroën.

5. References

[1] Vallet A and Borghi R., 1999 *C. R. Acad. Sci. Paris*, **327** ser II b 1015-1020
[2] Vallet A., Burluka A.A. and Borghi R., 2001 *Atomization and Spray*, **11** 619-642
[3] Reitz R.D. 1987 *Atomisation and Spray Technology* **3** 309-337
[4] Blokkeel G., Borghi R. and Barbeau B. 2003 *SAE Technical Paper* 2003-01-0005
[5] Marble F.E. and Broadwell J.E 1977 *Project Squid, Technical Report* **TRW-9-PU** Purdue University
[6] Burluka A.A. and Borghi R *Combustion*
[7] Stepowsky D. and Werquin O. 2002 *Combustion*, In press
[8] Carreau J.L., Monote G., Le Visage D. and Roger F. 1993 *Proc. ASME Winter Annual Meeting Spray Symposium* New Orleans
[9] Carreau J.L., Le Visage D., Monote G., Gicquel P. and Roger F. 1994 *ICLASS-94 Rouen* 94-101
[10] Prevost L., Carreau J.L., Porcheron E. and Roger F. 1999 *ILLASS Europe'99 Toulouse*
[11] Patankarand S.V. and Spalding D.B. 1970 *Morgan-Grampian* London
[12] Blokkeel G., Silvani X., Demoulin F.X. and Borghi R. 2002 *ILASS Europe, Zaragoza*
[13] F.Inc. 2001 *Fluent V6*
[14] Dumont N., Simonin O., Habchi C. 2000 *ILASS*
[15] Marcer R 2001 *Technical repport* G.S.M. D1.2
[16] Reitz R.D. 1996 *Spray Technology short course Pittsburgh PA*